A new toolbox to compare target localizations for non-invasive brain stimulation: An application of rTMS treatment for auditory hallucinations in schizophrenia

F. Briend, C. Nathou, N. Delcroix, S. Dollfus, Olivier M Etard

▶ **To cite this version:**

F. Briend, C. Nathou, N. Delcroix, S. Dollfus, Olivier M Etard. A new toolbox to compare target localizations for non-invasive brain stimulation: An application of rTMS treatment for auditory hallucinations in schizophrenia. Schizophrenia Research, 2020, 223, pp.305-310. 10.1016/j.schres.2020.09.001 . hal-03047850

HAL Id: hal-03047850

https://normandie-univ.hal.science/hal-03047850

Submitted on 14 Dec 2020

HAL is a multi-disciplinary open access archive for the deposit and dissemination of scientific research documents, whether they are published or not. The documents may come from teaching and research institutions in France or abroad, or from public or private research centers.

L'archive ouverte pluridisciplinaire **HAL**, est destinée au dépôt et à la diffusion de documents scientifiques de niveau recherche, publiés ou non, émanant des établissements d'enseignement et de recherche français ou étrangers, des laboratoires publics ou privés.

Title Page

A new toolbox to compare target localizations for non-invasive brain stimulation: An application of rTMS treatment for auditory hallucinations in schizophrenia

Briend F. PhD [a*], *Nathou C. MD/PhD* [a, b], *Delcroix N. PhD* [c], *Dollfus S. MD/PhD* [a, b], *Etard O. MD/PhD* [a d]

[a] Normandie Univ, UNICAEN, ISTS, EA 7466, GIP Cyceron, 14000 Caen, France

[b] CHU de Caen, Service de Psychiatrie adulte, Centre Esquirol, 14000 Caen, France

[c] Normandie Univ, UNICAEN, CNRS, CHU de Caen, UMS 3408, GIP Cyceron, 14000 Caen, France

[d] CHU de Caen, Service d'Explorations Fonctionnelles du Système Nerveux, 14000 Caen, France

* Corresponding author: Normandie Univ, UNICAEN, ISTS, EA 7466, GIP Cyceron, 14000 Caen, France. Tel.: +33 698101689; fax: +33 231065108.

E-mail : briend@cyceron.fr http://www.ists.cyceron.fr/

Abstract: 180 words

Text: 3500 words

Number of figures: 2 figures

ABSTRACT

Background: Most repetitive transcranial magnetic stimulation (rTMS) studies aiming to reduce auditory verbal hallucinations (AVH) in schizophrenia target the left temporo-parietal junction (TPJ), but the efficacy of this approach remains controversial. The observed differences in efficacy could be attributed to inaccurate target localization. Here, to precisely quantify anatomical bias induced by localization method, we developed a free open-source software (GeodesicSlicer) that computes shortest curved path (i.e. geodesic) between rTMS targets. Here we compare a personalized target with accurate anatomical criteria with a standardized target based on the 10-20 EEG system (the middle between T3 and P3 electrodes: T3P3).

Methods: We compare in 69 patients with schizophrenia the geodesic distances of two approaches for rTMS target localization within the left TPJ. In addition, we characterize the personalized target according to the 10-20 EEG system.

Results: A differential of 3 cm in term of geodesic distance between rTMS localization approaches was observed. Moreover, this personalized target to treat AVH is located at 25% in the T3-P3 axis.

Conclusions: This software for rTMS localization comparison demonstrates the difference between standardized and personalized rTMS target. This difference has the potential to explain a part of the dissonant clinical results found in previous rTMS studies.

Keywords

Schizophrenia; rTMS; T3P3; auditory verbal hallucinations; geodesic distance; software.

1. Introduction

Repetitive transcranial magnetic stimulation (rTMS) over the left temporo-parietal junction (TPJ) has emerged as a treatment to reduce auditory verbal hallucinations (AVH) in schizophrenia (Dollfus et al., 2016a; Hoffman et al., 1999, 2000). The TPJ is involved in both language processes and AVH (Kühn and Gallinat, 2012), however previous studies targeting rTMS to the left TPJ have reported inconsistent efficacies (Dollfus et al., 2016a; Kennedy et al., 2018; Montagne-Larmurier et al., 2011; Slotema et al., 2014). These inconsistencies could be due to the study design (sham condition or not, type of clinical study, the type of coil used, …) (Dollfus et al., 2016b), different stimulation frequency (Dollfus et al., 2018, 2016b), and inaccurate site determination, depending on different approaches to target the TPJ rTMS site (Donaldson et al., 2015; Sack et al., 2009). The TPJ is a supramodal association area, with no consensus on coordinates or anatomical landmarks (Bzdok et al., 2013). This large area contrasts with the sharp shape focality of the rTMS magnetic field (Cohen et al., 1990). Consequently, rTMS efficacy might be improved by a better target identification that might decrease the inter-subjects variability (Nathou et al., 2015; Ruohonen and Karhu, 2010). One way is to take into account the anatomical variability since previous reports have shown that the effects of the stimulation are proportional to the distance from the stimulation to the target (Cohen et al., 1990; Fadini et al., 2009). However, most clinical applications are based on standardized targeting methods that do not take into account for individual anatomy, which can contribute to suboptimal clinical responses compared to other methods such as personalized targeting techniques based on individual brain imaging (Herbsman and Nahas, 2011).

Currently, there are two methods for targeting the TPJ. On one hand, the Standardized Target method (ST) uses the standardized T3P3 site according to the International 10–20 system of electroencephalogram (EEG) electrode positioning (Jasper, 1958; Klem et al.,

1999). This site determination is widely applied for positioning the coil in the cognitive neurosciences and in psychiatric treatments, but is known to be a rough estimation, especially given its variable projections on the individual brain (Herwig et al., 2003). On the other hand, the Personalized Target (PT) method based on the magnetic resonance imaging (MRI) (Sommer et al., 2018, 2007) uses the subject's own structural or functional images to guide target placement (Herwig et al., 2001; Sack et al., 2009). While the findings of Sack and colleagues revealed a systematic behavioral difference between these TMS localization approaches (Sack et al., 2009), no tools allow to compare the rTMS site determination. Recently in a PT study, we observed a significant improvement of AVH after delivering rTMS at one accurate anatomical site (Dollfus et al., 2018). We therefore postulated that choosing ST using 10-20 EEG system over PT using anatomical landmarks could induce an anatomical bias able to explain clinical outcomes. In order to precisely quantify this anatomical bias, and because using different TMS targeting methods will lead to somewhat different scalp targets, we developed a free open-source software: GeodesicSlicer (Briend et al., 2020), that computes the shortest path at scalp-surface between any rTMS targets, whether localized by MRI-guided neuronavigation or by the 10-20 EEG system.

2. Material and methods

2.1. GeodesicSlicer: Toolbox for rTMS localization comparison

The ST localization corresponding to a particular scalp position (T3P3) and the PT localization determined by computerized cortical MRI scan must be in a common space to be properly compared. To reach this goal, we developed the open-source tool GeodesicSlicer (The code and description are available in the Wikipage) (Briend et al., 2020). This software is based on the geodesic distance measurement (defined as the shortest path between two points in a curved space) at scalp-surface calculated on a mesh morphed to participant-specific brain MRI. The provided toolbox creates 3D mesh morphed to the structural MRI

head data of the participant and implements Dijkstra's algorithm to calculate the shortest path to the vertices of a triangle on a mesh (Dijkstra, 1959). Thanks to the Dijkstra's algorithm and according to the international guidelines of the 10-20 EEG (Jasper, 1958; Klem et al., 1999), an individualized 10-20 system EEG was projected onto the head surface of the participant (see Fig. 1). Finally, the software calculates the geodesic distances between any given rTMS localizations. The guidelines to realize that is described in the toolbox documentation on our Wikipage (via the steps of the "Parameters to find the shortest path" module of the software: https://www.slicer.org/wiki/Documentation/Nightly/Modules/GeodesicSlicer#Parameters_to_find_the_shortest_path).

2.2. Standardized site determination (ST)

Sixty-nine T1-weighted images of schizophrenia patients (SZ; 37.81 ± 8.86 years; 26 women, DSM IV-TR (American Psychiatric Association, 2000)) recruited from our previous studies (Dollfus et al., 2018; Maïza et al., 2013; Montagne-Larmurier et al., 2011) were included to locate ST on their individual meshes.

Imaging was performed with a 3-Tesla scanner (Intera Achieva 3T, Philips Medical System, the Netherlands) to acquire a T_1-weighted whole-brain anatomical image [3D-FFE-TFE sequence; matrix size, 256 × 256 with 180 contiguous slices; field of view: 256 mm; isotropic resolution, 1 mm; sagittal slice orientation; repetition time: 20 ms; echo time: 4.6 ms; flip angle: 101°; inversion time: 800 ms; SENSE factor, 2].

Triangle meshes morphed to participant-specific MRI native space were reconstructed from the 69 T1-weighted whole-brain anatomical image using 3D Slicer software (Fedorov et al., 2012; Pieper et al., 2006) (http://www.slicer.org, "editor toolbox" version 4.10, implemented in GeodesicSlicer).Then four anatomical landmarks based on the standard landmarks of the skull used in the 10-20 system EEG were manually placed by a neuroimaging expert for the essential positioning of the electrodes: the nasion, the inion, and

the left and right tragi. Finally, the GeodesicSlicer toolbox reconstructed the 10-20 system EEG onto the head surface with T3P3 (here designated ST) in the center of the segment delimited by T3 and P3 according to the 10-20 electrode system of the International Federation (Jasper, 1958; Klem et al., 1999) (Fig. 1). For localization approaches comparison, each set of ST coordinates (n=69) were then individually transformed to a normalized stereotactic space (MNI) with SPM12 and plotted on the scalp of the MNI MRI single-subject mesh.

2.2.1. Validity of the measure

Eight controls (35.77 ± 5.29 years; 2 women) were included to assess the validity of the GeodesicSlicer method. The placement of the nasion, inion, and the two tragi determines the position of the electrodes in the 10-20 system EEG (Klem et al., 1999). We measured the distances from the nasion to the inion and from the left tragus and the right tragus in the controls with a measuring tape, as established in the 10-20 EEG guidelines (Klem et al., 1999), and compared them to the same distances calculated by GeodesicSlicer. A Bland–Altman plot was used to assess test reliability from these two measurements (Bland and Altman, 1999).

2.2.2. MNI Location of ST

An in-house MATLAB program was used to determine the anatomical appellation of the area corresponding to the ST and PT coordinates reported in the automated anatomical labeling (AAL) atlas of the MNI MRI single-subject brain (Tzourio-Mazoyer et al., 2002). The scalp position T3P3 was projected to the brain surface with the way how TMS effects project to the brain (i.e., perpendicular to the scalp-surface).

2.3. Personalized site determination (PT)

One parallel, randomized, double-blinded, and sham-controlled study using the PT method with significant AVH reduction was selected. This study reported a site anatomically determined at the crossing between the projection of the ascending branch of the left lateral sulcus and the left superior temporal sulcus named as PT_D (see Supplementary Data Video 1 in (Dollfus et al., 2018)). PT_D was first manually placed on the 69 T1-weighted images and then each location was individually transformed to a normalized stereotactic space (MNI) with SPM12. Each PT point (n=69) was then plotted on the scalp of the MNI MRI single-subject mesh (cf. Fig. 2).

2.4. Comparison of the PT and ST locations

We plotted the 95% confidence ellipsoids (Friendly et al., 2013) associated with the PT (n=69) and ST (n=69) distributions to characterize the PT and ST locations. Because PT and ST point distributions (D) followed normal distributions ($\mathcal{N}$), $D_{PT} \sim \mathcal{N}(\mu_{PT}, \Sigma_{PT})$ and $D_{ST} \sim \mathcal{N}(\mu_{ST}, \Sigma_{ST})$ in which μ is the center of mass of D and Σ is the covariance matrix of D, the confidence regions R(D) were computed as follows:

$$R = (D - \mu)'\Sigma^{-1}(D - \mu) \leq \frac{p}{(n-p)} F_{0.05,p,n-p} \qquad \textbf{(1)}$$

where F is the Fisher distribution, the dimensionality p = 3, and the number of target positions is designated as R_{PT} n=69 and R_{ST} n=69.

Hotelling's T^2-test (Hotelling, 1931) was used to test for differences in location between groups (PT *vs.* ST) at an alpha level of 0.05 (using the "Hotelling" package in R (Curran, 2017)). The geodesic distances between the centers of the two ellipsoids (μ_{PT}, μ_{ST}) were calculated to characterize the mean distance between PT and ST on the MNI MRI single-subject mesh and on each 69 participant-specific MRI native space meshes.

The geodesic distances between PT (μ_{PT}) and the T3 electrode and PT (μ_{PT}) and the P3 electrode were determined in order to describe the mean PT position in terms of the landmarks of a 10-20 system EEG.

All the geodesic distances were computed with GeodesicSlicer.

3. Results

3.1. Standardized site determination (ST)

3.1.1. Validity of the measure

The limits of agreement of Bland–Altman plots of the nasion-inion distances were from −0.82 to 1.96 cm, with a mean difference of both measures of 0.57 ± 0.70 cm (range, −0.64 to 1.59 cm), and from −0.52 to 1.82 cm for the tragus-tragus with a mean difference of 0.65 ± 0.59 cm (range, −0.16 to 1.53 cm), showing that the reliability between the measures calculated by GeodesicSlicer and manually was consistent.

3.1.2. MNI Location of ST

The standardized site determination showed that projected T3P3 targets were widespread: 1.44% points were in the left inferior parietal gyrus, 1.44% were in the left inferior temporal gyrus, 4.34% were in the left angular gyrus, 4.34% were in the left superior temporal gyrus, 30.43% were in the left supramarginal gyrus, and 57.97% were in the left middle temporal gyrus. In contrast for PT, 1.4% points were in the left supramarginal gyrus, 7.2% were in the left temporal superior gyrus and 91.3% were in the left temporal middle gyrus.

3.2. Comparison of the PT and ST locations

Figure 2 shows both PT and ST patterns and their confidence regions. No R_{PT} points (where μ_{PT}; x= -84.17, y= -39.12, z= 1.95) was contained in the confidence region of R_{ST} (where μ_{ST}; x= -77.39, y= -63.42, z=15.67). The group location difference was significant ($T^2_{3,134} = 1150.04$, $P < 0.001$), and PT was below and in front of ST at a distance of 3.01 cm on the MNI MRI single-subject mesh or at a mean of 2.95 ± 0.73 cm (n=69) on participant-specific MRI native space meshes.

In native spaces, the distances between on one hand PT (μ_{PT}) and T3 and on the other hand P3 and T3 were 2.76 ± 0.79 cm and 11.09 ± 0.90 cm, respectively, in the 10-20 system EEG. Thus, PT was located at the junction between the first and the second quarter of the T3P3 segment.

4. Discussion

Although hypothetical in nature, the highly variable TMS locations are causally related to inconsistent clinical outcomes in previous TMS-AVH studies. Here we demonstrate, thanks to a new and free open-source software (GeodesicSlicer) as a common easy-to-use software for rTMS localization comparison, a differential of nearly 3 cm (geodesic distance) between personalized rTMS target efficient on AVH (Dollfus et al., 2018) and the standardized T3P3 method. These 3 cm represent a large distance since the electric field induced by rTMS drops by more than two at a distance of 2 cm from the center of the coil in the brain tissue (Cohen et al., 1990; Fadini et al., 2009).

4.1. The T3P3 localization

The likelihood of experiencing AVH is influenced by impaired activity in the vicinity of the posterior part of the superior and middle temporal gyrus which is part of the TPJ (Kühn and Gallinat, 2012). However, the present results show that more than one third of ST locations were outside this focal area. The remaining two thirds of the ST sites were located over the left superior or middle temporal gyrus that borders the superior temporal sulcus, supporting the large variability of the location of ST and the fact that the stimulation target does not necessary correspond to the intended target. This is probably due to the large inter-individual anatomical variability (Herwig et al., 2003) and could explain the discrepancy in terms of efficacy when using ST (Dollfus et al., 2016a; Slotema et al., 2014). These results support the need for more precise rTMS localization.

4.2. The personalized target localization

Recent findings suggest that focal brain stimulation should be guided in a personalized manner (Lahti, 2016; Sommer et al., 2018) since personalized medicine for the treatment of psychosis allows for the consideration of substantial inter-individual variability (Lahti, 2016). Interestingly, recent parallel, randomized, double-blinded, and sham-controlled studies in

which rTMS was delivered by individualized neuronavigation over the left superior temporal sulcus (separating the superior temporal gyrus from the middle temporal gyrus, both regions imply in AVH (Kühn and Gallinat, 2012)) around the Wernicke's area showed consistent AVH improvements (Dollfus et al., 2018; Hoffman et al., 2013; Kindler et al., 2013). In contrast, a clinical trial that directly compared the 10-20 method with a personalized method guided by maximal fMRI activation did not find superiority of the personalized method and did not even find superiority to sham stimulation (Slotema et al., 2011). In the same way, another research team used neuronavigation systems integrating morphological and functional imaging data to determine that Heschl's gyrus as the stimulation target rather than Wernicke's area (Blumberger et al., 2012). AVHs were not significantly improved in that study, probably because Heschl's gyrus is in the depth of the lateral sulcus and above and in front of Wernicke's region. Taken together, these findings highlights the importance of accurate rTMS site determination, and enlighten Wernicke's region seems to be a site-optimized protocol for some clinical benefit in patients with persistent AVH (Donaldson et al., 2015; Hoffman et al., 2013). In addition to anatomical variability, rTMS efficacy could also be related to different frequencies and study designs used (Dollfus et al., 2018, 2016b). A strong effort to individualize these approaches should have be done, as for example calculating the correction factors for each patient to adjust the rTMS dose for the treatment (Briend et al., 2020).

In addition to the inter-individual differences found with the T3P3 method, these results clearly indicate a need for better and more accessible localization techniques for rTMS optimization. We determined an accurate anatomical site in the left TPJ within the left Wernicke's region considered to be the best region for stimulation to reduce AVH (Hoffman et al., 2007) that can be easily identified and reproducible in clinical practice (Dollfus et al., 2018). It is close to the PT sites used in other studies reporting rTMS efficacy for the reduction of AVH (Hoffman et al., 2013), supporting the fact that the posterior part of the left

STG is a relevant region for AVH treatment by rTMS (Dollfus et al., 2018; Hoffman et al., 2013; Montagne-Larmurier et al., 2011).

Our results also suggest that a stimulation target around the junction between the first and the second quarter of the T3P3 segment should be used when individualized methods based on neuroimaging techniques and/or neuronavigation system are not available. However, it is important to remember that ST does not account for inter-subject differences in cortical anatomy or skull size.

4.3. GeodesicSlicer

GeodesicSlicer is implemented as a free extension of the widely used 3D Slicer medical image visualization and analysis application platform (http://www.slicer.org (Fedorov et al., 2012; Pieper et al., 2006)). GeodesicSlicer uses cortical stimulation target from either functional or anatomical image to provide functionality specifically designed for Non-invasive brain stimulation therapy research. This module can compute geodesic paths between any rTMS targets, whether localized by MRI-guided TMS neuronavigation or localized by 10-20 EEG position. Based on Andoh's triangulation-based MRI-guided method (Andoh et al., 2009), this module could also calculates the geodesic distances between the projected stimulation target and the position of the 3 nearest electrodes in the individualized 10-20 system EEG in order to guide the stimulation (Briend et al., 2020). Please refer to the toolbox documentation on our Wikipage for detailed steps. This method provides a reliable and inexpensive way to position the TMS coil that can be used in case of unavailable online neuronavigation like in a clinical setting (Briend et al., 2020), but also in comparing different localizations due to different target modalities via the "Parameters to find the shortest path" module of the software. For any sort of questions, feedback, suggestions, or critique, please visit the 3D slicer support forum.

4.4. Study limitations

This study has some limitations. First, the different ST and PT locations were not analyzed in view of clinical outcomes, highlighting the need for further prospective and controlled studies. Second, the ST location was not directly located on the subject head but was calculated with Dijkstra's algorithm via GeodesicSlicer and then was compared with PT target. The path precision calculated by the Dijkstra's algorithm depends on the length of the triangle edges determined by the number of triangles created during the mesh generation and could add some variability. However, the triangle size is low compared to the difference found between the two approaches for rTMS target localization and the Bland-Altman plot showed a good reliability of GeodesicSlicer. Moreover, we compared ST and PT exact points, but it would have been good to evaluate if previous ST studies place or not the magnetic coil exactly on top of T3P3 or little more anteriorly to that point to reach more posterior part of the temporal gyrus, but usually no precise descriptions, like MNI coordinates, was given in the ST studies (Dollfus et al., 2016a).

5. Conclusions

In summary, the discrepant efficacy results previously reported in rTMS studies (Slotema et al., 2014) may be related to the choice of a generic target site located at T3P3 (Fitzgerald et al., 2005; Herwig et al., 2003), which does not necessarily overlap with the left language areas involved in AVH (Hoffman et al., 2000; Kühn and Gallinat, 2012). It is why we propose a new and free open-source software (GeodesicSlicer) as a common easy-to-use software for rTMS localization comparison.

Acknowledgements: The authors would like to thank A. Nourry, Dr. A. Lasso and Dr. K. Yoshimi for their valuable help with the VTK library.

Conflict of interest: The authors have no conflicts of interest to declare.

Funding source: This work was supported by a Perceneige-Fondamental foundation prize, the French Health Ministry (Programme Hospitalier de Recherche Clinique), Normandie Council and Univeristy of Caen.

6. References

American Psychiatric Association, 2000. Diagnostic and statistical manual of mental disorders (4th ed., text rev.), American Psychiatric Publishing. ed. Washington, DC: American Psychiatric Association.

Andoh, J., Riviere, D., Mangin, J.F., Artiges, E., Cointepas, Y., Grevent, D., Paillere-Martinot, M.L., Martinot, J.L., Cachia, A., 2009. A triangulation-based magnetic resonance image-guided method for transcranial magnetic stimulation coil positioning. Brain Stimul 2, 123–31. https://doi.org/10.1016/j.brs.2008.10.002

Bland, J.M., Altman, D.G., 1999. Measuring agreement in method comparison studies. Stat. Methods Med. Res. 8, 135–160.

Blumberger, D.M., Christensen, B.K., Zipursky, R.B., Moller, B., Chen, R., Fitzgerald, P.B., Daskalakis, Z.J., 2012. MRI-targeted repetitive transcranial magnetic stimulation of Heschl's gyrus for refractory auditory hallucinations. Brain Stimulat. 5, 577–585. https://doi.org/10.1016/j.brs.2011.12.002

Briend, F., Leroux, E., Nathou, C., Delcroix, N., Dollfus, S., Etard, O., 2020. GeodesicSlicer: a Slicer Toolbox for Targeting Brain Stimulation. Neuroinformatics. https://doi.org/10.1007/s12021-020-09457-9

Bzdok, D., Langner, R., Schilbach, L., Jakobs, O., Roski, C., Caspers, S., Laird, A.R., Fox, P.T., Zilles, K., Eickhoff, S.B., 2013. Characterization of the temporo-parietal junction by combining data-driven parcellation, complementary connectivity analyses, and functional decoding. NeuroImage 81, 381–392. https://doi.org/10.1016/j.neuroimage.2013.05.046

Cohen, L.G., Roth, B.J., Nilsson, J., Dang, N., Panizza, M., Bandinelli, S., Friauf, W., Hallett, M., 1990. Effects of coil design on delivery of focal magnetic stimulation. Technical

considerations. Electroencephalogr. Clin. Neurophysiol. 75, 350–357. https://doi.org/10.1016/0013-4694(90)90113-X

Curran, J.M., 2017. R Package "Hotelling."

Dijkstra, E.W., 1959. A note on two problems in connexion with graphs. Numer. Math. 1, 269–271. https://doi.org/10.1007/BF01386390

Dollfus, S., Jaafari, N., Guillin, O., Trojak, B., Plaze, M., Saba, G., Nauczyciel, C., Montagne Larmurier, A., Chastan, N., Meille, V., Krebs, M.-O., Ayache, S.S., Lefaucheur, J.P., Razafimandimby, A., Leroux, E., Morello, R., Marie Batail, J., Brazo, P., Lafay, N., Wassouf, I., Harika-Germaneau, G., Guillevin, R., Guillevin, C., Gerardin, E., Rotharmel, M., Crépon, B., Gaillard, R., Delmas, C., Fouldrin, G., Laurent, G., Nathou, C., Etard, O., 2018. High-Frequency Neuronavigated rTMS in Auditory Verbal Hallucinations: A Pilot Double-Blind Controlled Study in Patients With Schizophrenia. Schizophr. Bull. 44, 505–514. https://doi.org/10.1093/schbul/sbx127

Dollfus, S., Lecardeur, L., Morello, R., Etard, O., 2016a. Placebo Response in Repetitive Transcranial Magnetic Stimulation Trials of Treatment of Auditory Hallucinations in Schizophrenia: A Meta-Analysis. Schizophr. Bull. 42, 301–308. https://doi.org/10.1093/schbul/sbv076

Dollfus, S., Lecardeur, L., Morello, R., Etard, O., 2016b. Placebo Response in Repetitive Transcranial Magnetic Stimulation Trials of Treatment of Auditory Hallucinations in Schizophrenia: A Meta-Analysis. Schizophr. Bull. 42, 301–308. https://doi.org/10.1093/schbul/sbv076

Donaldson, P.H., Rinehart, N.J., Enticott, P.G., 2015. Noninvasive stimulation of the temporoparietal junction: A systematic review. Neurosci. Biobehav. Rev. 55, 547–572. https://doi.org/10.1016/j.neubiorev.2015.05.017

Fadini, T., Matthäus, L., Rothkegel, H., Sommer, M., Tergau, F., Schweikard, A., Paulus, W., Nitsche, M.A., 2009. H-coil: Induced electric field properties and input/output curves on healthy volunteers, comparison with a standard figure-of-eight coil. Clin. Neurophysiol. 120, 1174–1182. https://doi.org/10.1016/j.clinph.2009.02.176

Fedorov, A., Beichel, R., Kalpathy-Cramer, J., Finet, J., Fillion-Robin, J.-C., Pujol, S., Bauer, C., Jennings, D., Fennessy, F., Sonka, M., Buatti, J., Aylward, S., Miller, J.V., Pieper, S., Kikinis, R., 2012. 3D Slicer as an image computing platform for the Quantitative Imaging Network. Magn. Reson. Imaging, Quantitative Imaging in Cancer 30, 1323–1341. https://doi.org/10.1016/j.mri.2012.05.001

Fitzgerald, P.B., Benitez, J., Daskalakis, J.Z., Brown, T.L., Marston, N.A.U., de Castella, A., Kulkarni, J., 2005. A double-blind sham-controlled trial of repetitive transcranial magnetic stimulation in the treatment of refractory auditory hallucinations. J. Clin. Psychopharmacol. 25, 358–362.

Friendly, M., Monette, G., Fox, J., 2013. Elliptical Insights: Understanding Statistical Methods through Elliptical Geometry. Stat. Sci. 28, 1–39. https://doi.org/10.1214/12-STS402

Herbsman, T., Nahas, Z., 2011. Anatomically based targeting of prefrontal cortex for rTMS. Brain Stimulat. 4, 300–302. https://doi.org/10.1016/j.brs.2011.01.004

Herwig, U., Satrapi, P., Schönfeldt-Lecuona, C., 2003. Using the international 10-20 EEG system for positioning of transcranial magnetic stimulation. Brain Topogr. 16, 95–99.

Herwig, U., Schönfeldt-Lecuona, C., Wunderlich, A.P., von Tiesenhausen, C., Thielscher, A., Walter, H., Spitzer, M., 2001. The navigation of transcranial magnetic stimulation. Psychiatry Res. 108, 123–131.

Hoffman, R.E., Boutros, N.N., Berman, R.M., Roessler, E., Belger, A., Krystal, J.H., Charney, D.S., 1999. Transcranial magnetic stimulation of left temporoparietal cortex in three patients reporting hallucinated "voices." Biol. Psychiatry 46, 130–132.

Hoffman, R.E., Boutros, N.N., Hu, S., Berman, R.M., Krystal, J.H., Charney, D.S., 2000. Transcranial magnetic stimulation and auditory hallucinations in schizophrenia. The Lancet 355, 1073–1075. https://doi.org/10.1016/S0140-6736(00)02043-2

Hoffman, R.E., Hampson, M., Wu, K., Anderson, A.W., Gore, J.C., Buchanan, R.J., Constable, R.T., Hawkins, K.A., Sahay, N., Krystal, J.H., 2007. Probing the pathophysiology of auditory/verbal hallucinations by combining functional magnetic resonance imaging and transcranial magnetic stimulation. Cereb. Cortex N. Y. N 1991 17, 2733–2743. https://doi.org/10.1093/cercor/bhl183

Hoffman, R.E., Wu, K., Pittman, B., Cahill, J.D., Hawkins, K.A., Fernandez, T., Hannestad, J., 2013. Transcranial magnetic stimulation of Wernicke's and right homologous sites to curtail "voices:" a randomized trial. Biol. Psychiatry 73, 1008–1014. https://doi.org/10.1016/j.biopsych.2013.01.016

Hotelling, H., 1931. The Generalization of Student's Ratio. Ann. Math. Stat. 2, 360–378. https://doi.org/10.1214/aoms/1177732979

Jasper, H., 1958. The ten twenty electrode system of the international federation. Electroencephalogr. Clin. Neurophysiol. 10, 371–375.

Kennedy, N.I., Lee, W.H., Frangou, S., 2018. Efficacy of non-invasive brain stimulation on the symptom dimensions of schizophrenia: A meta-analysis of randomized controlled trials. Eur. Psychiatry J. Assoc. Eur. Psychiatr. 49, 69–77. https://doi.org/10.1016/j.eurpsy.2017.12.025

Kindler, J., Homan, P., Jann, K., Federspiel, A., Flury, R., Hauf, M., Strik, W., Dierks, T., Hubl, D., 2013. Reduced Neuronal Activity in Language-Related Regions After

Transcranial Magnetic Stimulation Therapy for Auditory Verbal Hallucinations. Biol. Psychiatry 73, 518–524. https://doi.org/10.1016/j.biopsych.2012.06.019

Klem, G.H., Lüders, H.O., Jasper, H.H., Elger, C., 1999. The ten-twenty electrode system of the International Federation. The International Federation of Clinical Neurophysiology. Electroencephalogr. Clin. Neurophysiol. Suppl. 52, 3–6.

Kühn, S., Gallinat, J., 2012. Quantitative Meta-Analysis on State and Trait Aspects of Auditory Verbal Hallucinations in Schizophrenia. Schizophr. Bull. 38, 779–786. https://doi.org/10.1093/schbul/sbq152

Lahti, A.C., 2016. Making Progress Toward Individualized Medicine in the Treatment of Psychosis. Am. J. Psychiatry 173, 5–7. https://doi.org/10.1176/appi.ajp.2016.15101320

Maïza, O., Hervé, P.-Y., Etard, O., Razafimandimby, A., Montagne-Larmurier, A., Dollfus, S., 2013. Impact of Repetitive Transcranial Magnetic Stimulation (rTMS) on Brain Functional Marker of Auditory Hallucinations in Schizophrenia Patients. Brain Sci. 3, 728–743. https://doi.org/10.3390/brainsci3020728

Montagne-Larmurier, A., Etard, O., Maïza, O., Dollfus, S., 2011. Repetitive transcranial magnetic stimulation in the treatment of auditory hallucinations in schizophrenic patients. Curr. Opin. Psychiatry 24, 533–540. https://doi.org/10.1097/YCO.0b013e32834bd26e

Nathou, C., Simon, G., Dollfus, S., Etard, O., 2015. Cortical Anatomical Variations and Efficacy of rTMS in the Treatment of Auditory Hallucinations. Brain Stimulat. 8, 1162–1167. https://doi.org/10.1016/j.brs.2015.06.002

Pieper, S., Lorensen, B., Schroeder, W., Kikinis, R., 2006. The NA-MIC Kit: ITK, VTK, pipelines, grids and 3D slicer as an open platform for the medical image computing community, in: 3rd IEEE International Symposium on Biomedical Imaging: Nano to

Macro, 2006. Presented at the 3rd IEEE International Symposium on Biomedical Imaging: Nano to Macro, 2006., pp. 698–701. https://doi.org/10.1109/ISBI.2006.1625012

Ruohonen, J., Karhu, J., 2010. Navigated transcranial magnetic stimulation. Neurophysiol. Clin. Clin. Neurophysiol. 40, 7–17. https://doi.org/10.1016/j.neucli.2010.01.006

Sack, A.T., Cohen Kadosh, R., Schuhmann, T., Moerel, M., Walsh, V., Goebel, R., 2009. Optimizing functional accuracy of TMS in cognitive studies: a comparison of methods. J. Cogn. Neurosci. 21, 207–221. https://doi.org/10.1162/jocn.2009.21126

Slotema, C.W., Blom, J.D., de Weijer, A.D., Diederen, K.M., Goekoop, R., Looijestijn, J., Daalman, K., Rijkaart, A.-M., Kahn, R.S., Hoek, H.W., Sommer, I.E.C., 2011. Can Low-Frequency Repetitive Transcranial Magnetic Stimulation Really Relieve Medication-Resistant Auditory Verbal Hallucinations? Negative Results from a Large Randomized Controlled Trial. Biol. Psychiatry, Schizophrenia: From Circuit Dysfunction to Treatment? 69, 450–456. https://doi.org/10.1016/j.biopsych.2010.09.051

Slotema, C.W., Blom, J.D., van Lutterveld, R., Hoek, H.W., Sommer, I.E.C., 2014. Review of the Efficacy of Transcranial Magnetic Stimulation for Auditory Verbal Hallucinations. Biol. Psychiatry 76, 101–110. https://doi.org/10.1016/j.biopsych.2013.09.038

Sommer, I.E., Kleijer, H., Hugdahl, K., 2018. Toward personalized treatment of hallucinations. Curr. Opin. Psychiatry 31, 237–245. https://doi.org/10.1097/YCO.0000000000000416

Sommer, I.E.C., de Weijer, A.D., Daalman, K., Neggers, S.F., Somers, M., Kahn, R.S., Slotema, C.W., Blom, J.D., Hoek, H.W., Aleman, A., 2007. Can fMRI-guidance improve the efficacy of rTMS treatment for auditory verbal hallucinations? Schizophr. Res. 93, 406–408. https://doi.org/10.1016/j.schres.2007.03.020

Tzourio-Mazoyer, N., Landeau, B., Papathanassiou, D., Crivello, F., Etard, O., Delcroix, N., Mazoyer, B., Joliot, M., 2002. Automated anatomical labeling of activations in SPM using a macroscopic anatomical parcellation of the MNI MRI single-subject brain. NeuroImage 15, 273–289. https://doi.org/10.1006/nimg.2001.0978

7. Figures

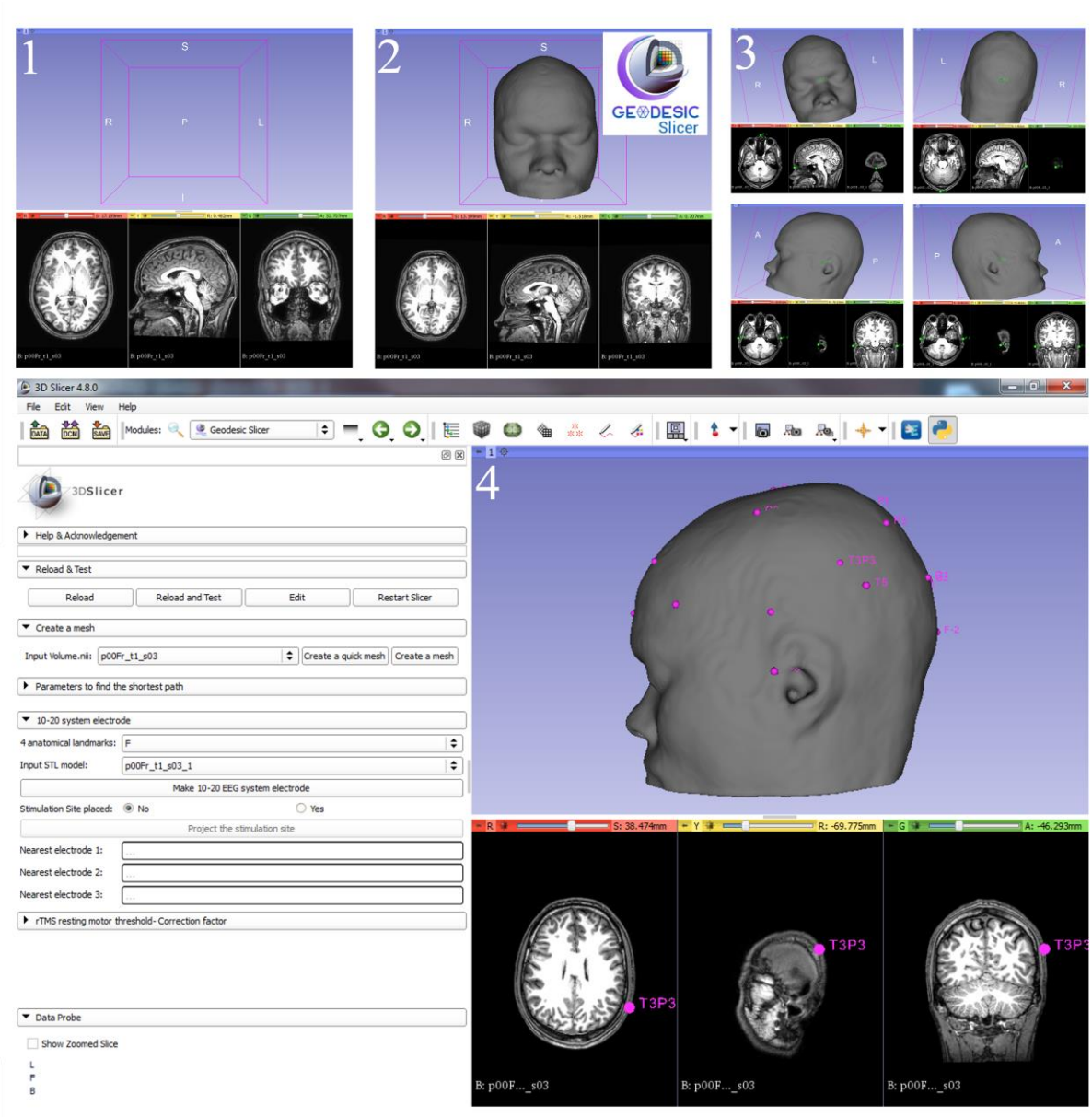

Fig. 1. *Screen-shot of the GeodesicSlicer program. The user: 1) Enters the T_1-weighted whole-brain anatomical image 2) Creates the triangle mesh 3) Places four anatomical landmarks: the nasion, the inion, the left tragus and the right tragus. 4) Executes the program that creates 3D mesh morphed to the structural MRI data of the participant and calculates the 10-20 system EEG with T3P3. Geodesic distances are computerizes from the "Parameters to find the shortest path" widget.*

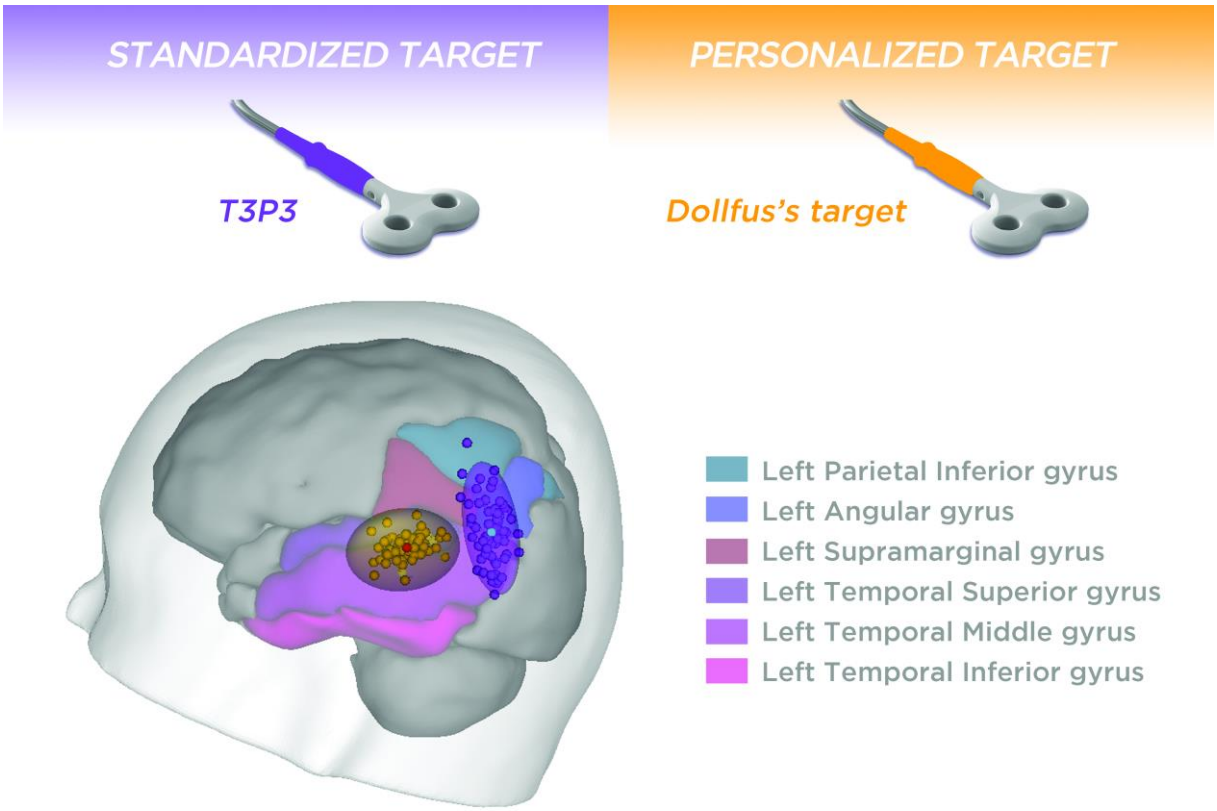

Fig. 2. *3D mesh morphed from the structural MNI MRI single-subject brain with different rTMS targets. Purple: the MNI location of the standardized target (T3P3, n=69) for which center is in cyan and given by x= -77.39, y= -63.42, z= 15.67. Orange: the MNI location of Dollfus's target (n=69) for which center is in red and given by x= -84.17, y= -39.12, z= 1.95 (once projected). Ellipsoids represent 95% confidence regions associated with distributions of personalized targets in yellow and standardized targets in purple.*